Polymer Bulletin (2026) 83:247
https://doi.org/10.1007/s00289-026-06294-9

ORIGINAL PAPER

Effect of pectin biopolymer addition on the mechanical, dynamic, and water absorption behavior of natural fiber-reinforced epoxy composites

R. Ashok Gandhi[1] · V. Jayaseelan[2] · S. Sambath[3] · Vijay Ananth Suyamburajan[4]

Received: 4 June 2025 / Revised: 18 August 2025 / Accepted: 2 January 2026

Abstract

The demand for sustainable, high-performance composites has created a need for natural fiber–reinforced systems with improved mechanical, durability, and environmental resistance properties. This study addresses this gap by developing epoxy-based composites reinforced with 30 vol% areca nut fiber and varying pectin filler contents from *Passiflora edulis* husks, with both reinforcements silane-treated to enhance fiber–matrix adhesion. Mechanical tests showed that the optimum formulation achieved ~28% higher tensile strength, ~24% higher flexural strength, and improved impact energy compared to the unfilled fiber composite. Fatigue life exceeded 27,000 cycles at 25% and 50% UTS, indicating strong cyclic load tolerance. Higher filler content enhanced hardness and creep resistance but resulted in a ~35% increase in water absorption. SEM analysis confirmed uniform filler dispersion and minimal interfacial gaps, correlating with the mechanical improvements. These results demonstrate that targeted filler loading can balance strength, durability, and moisture resistance, making the composites promising for demanding industrial applications.

Keywords Composites · Fibres · Biopolymers · Silane treatments · Water absorption

✉ R. Ashok Gandhi
ashokgandhir@gmail.com; ashokgandhir@hotmail.com

[1] Department of Mechanical Engineering, Sri Sai Ram Engineering College , Chennai 600044, India

[2] Department of Mechanical Engineering, Saveetha Engineering College, Chennai 602105, India

[3] Department of Mechanical Engineering, SRM Madurai College for Engineering and Technology, Pottapalayam 630612, Sivaganga District, Tamil Nadu, India

[4] Department of Mechanical Engineering, VELS Institute of Science, Technology & Advanced Studies, Chennai 600117, Tamil Nadu, India

Published online: 04 February 2026

Abbreviations

SEM	Scanning Electron Microscopy
MPa	Megapascal
VHN	Vickers hardness number
PLA	Polylactic acid
3-APTMS	3-Aminopropyltrimethoxysilane
UTS	Ultimate tensile strength
LLDPE	Linear low-density polyethylene
J	Joule
Vol. %	Volume percentage
ASTM	American Society for Testing and Materials

Introduction

The growing demand for sustainable and eco-friendly materials has increased interest in natural fibers for polymer composites. These fibers offer low density, biodegradability, and favorable mechanical properties, making them attractive for applications in packaging, construction, and automotive sectors [1]. Among them, areca nut fiber—extracted from the outer husk of the areca palm (*Areca catechu*)—is notable for its high cellulose, lignin, and hemicellulose content, which contribute to excellent tensile properties and suitability for load-bearing and semi-structural applications.

Previous studies have demonstrated the potential of areca fiber in enhancing composite performance. Ramanan et al. [2] reported that adding 20 vol% areca fiber and filler improved hardness to 74.14 VHN and tensile strength to 66.32 MPa. Sakib et al. [3] achieved tensile strengths up to 20.38 MPa for betel nut–reinforced epoxy composites. These findings highlight the ability of lignocellulosic reinforcements to improve stiffness, strength, and wear resistance.

Despite these advantages, natural fiber composites often face drawbacks such as void formation, poor fiber–matrix adhesion, and high moisture uptake [4, 5]. Incorporating fillers can mitigate these challenges by enhancing interfacial bonding and load transfer [6]. Pectin, a biopolymer extracted from *Passiflora edulis* husks, is rich in galacturonic acid and provides hydrophilic functional groups for better interaction with the polymer matrix [7]. It also offers biodegradability, low toxicity, and potential for thermal insulation applications. However, studies on the use of pectin as a structural filler in epoxy composites remain limited in literature.

Surface modification with silane coupling agents is a proven method to improve compatibility between hydrophilic reinforcements and hydrophobic matrices. 3-Aminopropyltrimethoxysilane (3-APTMS) is especially effective in forming covalent bonds with both filler and matrix, thereby improving interfacial adhesion. Balguri et al. [8] and Anžlovar et al. [9] reported significant gains in tensile and flexural strengths in silane-treated natural fiber composites, confirming the treatment's effectiveness in enhancing mechanical properties.Surface modification improves the interfacial adhesion of the composites [10].

Research gap and novelty

Although silane treatment is well-established for improving natural fiber–epoxy compatibility, the combined use of silane-treated areca nut fiber and pectin from *Passiflora edulis* husks has not been systematically explored for mechanical, fatigue, creep, and water absorption performance. This study addresses this gap by optimizing filler loading and surface treatment to produce a composite with improved strength, durability, and environmental resistance, suitable for marine, construction, and lightweight automotive applications.

Experimental procedure

Areca nut shells were obtained from Srinidi Trading, Chennai, India, and mechanically ground into short fibers with an average length of 5–10 mm and diameter of 80–120 μm. The density of the fibers was 1.23 g/cm³. The shells contained approximately 35–40 wt% cellulose, 25–28 wt% hemicellulose, and 28–32 wt% lignin, with trace extractives and ash.Pectin biopolymer derived from *Passiflora edulis* husks was procured from Adithya Chemicals, Chennai, India. The pectin had a degree of esterification of ~ 70%, purity > 98%, and moisture content < 8 wt%, with a density of 1.50 g/cm³.Epoxy resin LY556 (diglycidyl ether of bisphenol-A, density 1.16 g/cm³, epoxy equivalent weight 182–192 g/eq, viscosity 10,000–12,000 mPa·s at 25 °C) and curing agent HY951 (triethylenetetramine, density 0.97 g/cm³, amine value 480–520 mg KOH/g, viscosity 20–40 mPa·s at 25 °C) were obtained from Shield Solutions, Chennai, India.Silane coupling agent 3-aminopropyltrimethoxysilane (3-APTMS, purity ≥ 98%, density 1.03 g/cm³) and absolute ethanol (purity ≥ 99.9%, density 0.79 g/cm³) were supplied by Triveni Chemicals, Chennai, India. Both areca nut fibers and pectin filler were silane-treated before composite fabrication.

Fiber extraction from areca nuts

The following steps outline the technique for extracting areca nut fiber, which was used in this research. Figure 1 shows the many steps of the extraction process. The purchased areca nut shell was first washed under distilled water. Then dried under sunlight for exclude the moisture content. By using hammer mill fiber extractor (Model: HM-FE-5), the dried fiber is separated from the fruit husk. In order to eliminate any further dust contaminants, it is washed under distilled water and dried out by using hot air oven for period of 4 h at temperature of 90 ℃ [11]. Now the extracted fiber is processed further for better reinforcement over matrix.

Extraction of *Passiflora edulis* husk derived pectin

Before being dried in an oven at 80 ℃ for five hours, the passion fruit husks were rinsed with distilled water, sliced into small pieces, and blanched for five minutes to kill any pectin-degrading enzymes. Afterwards, a high-speed grinder was used to break the dry husks into powder. In order to aid in the breakdown of cell walls and

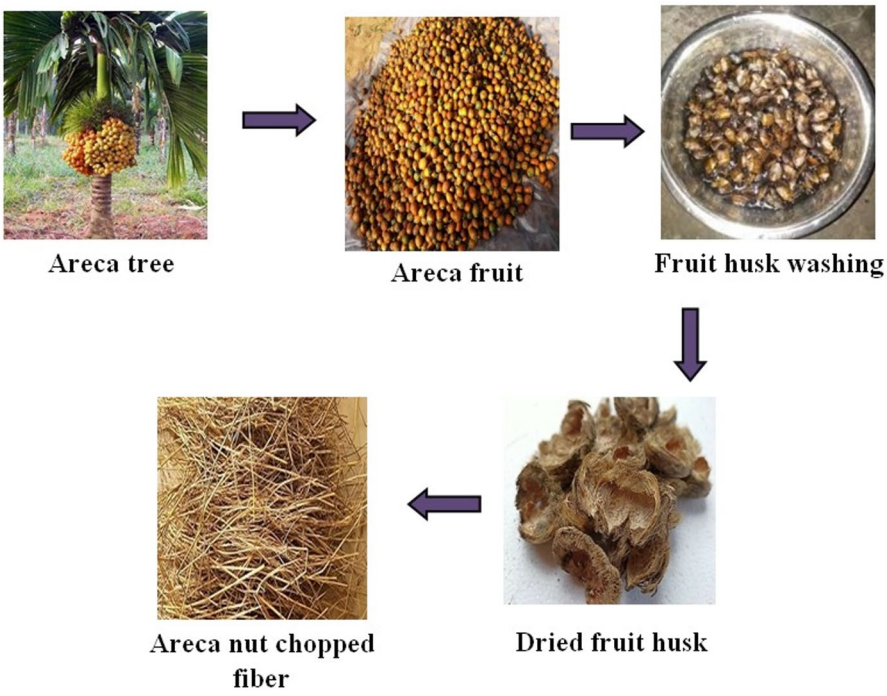

Fig. 1 Shows the many steps involved in extracting areca nut fiber

the release of pectin, the husk powder was combined with hydrochloric acid while stirring continuously to maintain a pH around 4 [12]. After 80 min of heating in a water bath at 75 °C, the pectin was extracted from the mixture. The liquid extract was then separated using vacuum filtering. The pectin was precipitated after 5 h of undisturbed addition of an equal volume of ethanol to the filtrate; centrifugation at 500 rpm for 15 min recovered the pectin. In the end, the pectin filler that had precipitated was dried in a laboratory oven set at 70 °C for a duration of three hours. Figure 2 illustrates the pectin synthesis process. Figure 3 presents SEM micrograph of synthesised pectin biopolymer obtained from *Passiflora edulis* husks, showing irregularly shaped agglomerated particles (A)with rough surface morphology (B) and abundant micropores (C). These morphological features are expected to increase the specific surface area and improve interfacial bonding when incorporated into the composite matrix. Scale bar = 2 μm.

Surface treatment process

Silane treatment was performed to improve the interfacial bonding between the epoxy matrix and the reinforcements (fiber and filler). A 2 wt% 3-aminopropyltrimethoxysilane (3-APTMS) solution was prepared by first dissolving the silane in water, then mixing it separately with ethanol. Acetic acid was added to adjust the pH to 4. The fibers and fillers were individually immersed in the silane solution and stirred

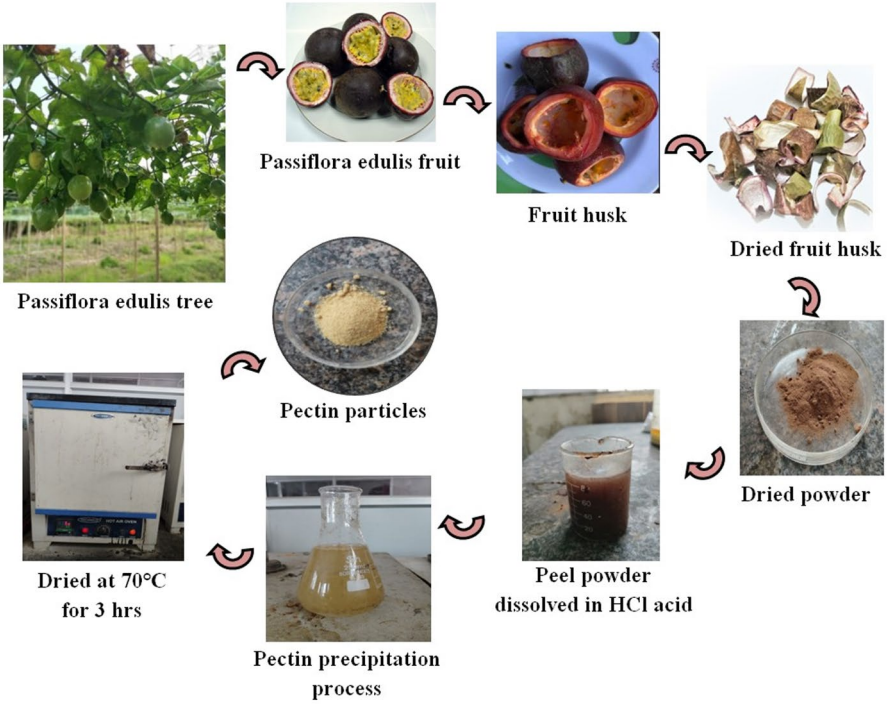

Fig. 2 Procedure for *Passiflora edulis* pectin extraction

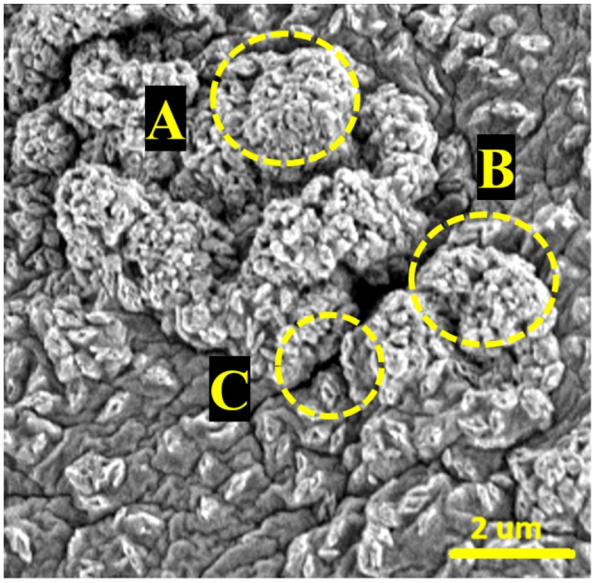

Fig. 3 Field Emission Scanning Microscope (FESEM) of a pectin biopolymer

continuously to ensure uniform coating [13]. The soaking process was maintained at room temperature (≈ 25 °C) for 6 h. After soaking, the reinforcements were rinsed with clean water to remove excess silane, followed by drying in a hot-air oven at 60 °C for 2.5 h. Figure 4 illustrates the silane treatment procedure.

Fabrication of composites

The matrix and its consistent hardener, triethylenetetramine, were combined in a 10:1 (w/w) ratio, and the two components were then thoroughly blended to create a homogenous solution. To avoid lumps and uneven distribution, the produced mixture was slowly added to the chopped areca nuts and pectin while being constantly stirred with a mechanical stirrer that had been coated with silane. Pouring the slurry into a clean mold that had been treated with a releasing agent made demolding the finished product after it had cured much easier [26]. The hand lay-up method was used to increase consolidation and surface smoothness when fabricating composite panels. The composites were post-cured for three hours at 70 °C in a hot air oven after being cured for 23 h at room temperature to boost their mechanical strength. Table 1 displays the reinforcing concentration. In Fig. 5, the composite plate is shown.

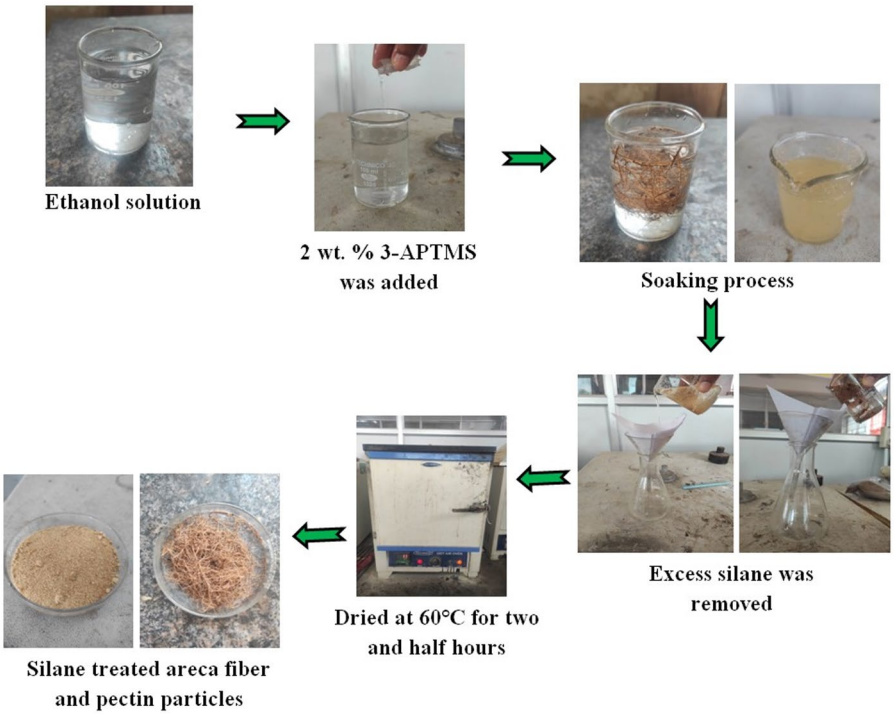

Fig. 4 Silane process for reinforcing fibers and fillers

Table 1 Composite sample codes, composition ranges, and total reinforcement content

Specimen labels	Reinforcements	Total reinforcement content (Vol. %)
R	100 Vol. % epoxy resin	0
RA	70 Vol. % epoxy resin + 30 Vol. % areca nut fiber	30
RAP0	69 Vol. % epoxy resin + 30 Vol. % areca nut fiber + 1 Vol. % pectin	31
RAP1	67 Vol. % epoxy resin + 30 Vol. % areca nut fiber + 3 Vol. % pectin	33
RAP2	65 Vol. % epoxy resin + 30 Vol. % areca nut fiber + 5 Vol. % pectin	35

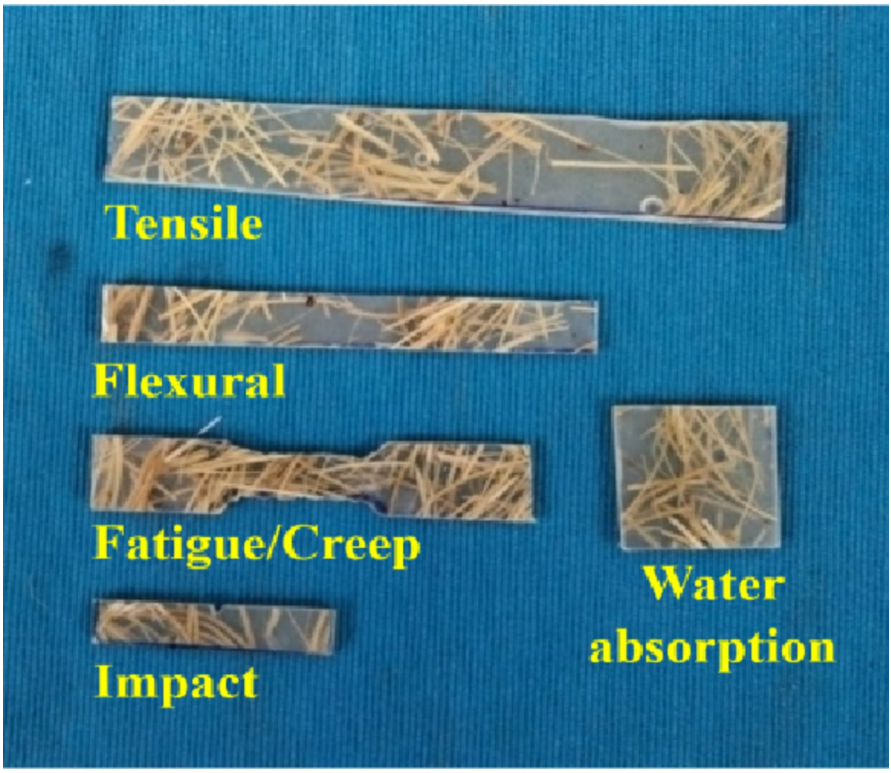

Fig. 5 Test specimens of the composite RA

Testing of composite and their details

In order to get the specimen ready for testing, the manufactured laminates were cut to standard proportions with a water abrasive jet cutting machine. This study used mechanical, fatigue, creep, and water absorption testing. Five specimens were tested for each test.

Mechanical strength

The composite's strength, stiffness, and deformation resistance were measured using conventional test methods. Using the following standards: ASTM D3039 for tensile testing, D790 for flexural testing, D2240 for hardness testing, and D256 for impact testing. Tests for tensile strength and elongation at break were conducted on specimens shaped like dumbbells using a universal testing machine. In order to find the modulus and flexural strength, rectangular specimens were bent in three different directions. The hardness test was carried out using a digital shore-D hardness tester to provide information about the material's resistance to targeted surface deformation. To evaluate impact resistance, a Charpy impact tester was used to determine the energy absorbed during rapid fracture.

Fatigue strength

The fatigue performance of the composites was assessed at ambient conditions (≈25 °C) using a rotational bending fatigue apparatus, following the guidelines of ASTM D3479.Specimens were subjected to a constant amplitude cyclic loading with a stress ratio ($R=0.1$). Load levels were set at 80%, 70%, and 60% of the ultimate tensile strength (UTS) obtained from static tensile tests. The number of cycles to failure (*Nf*) was recorded for each load level. The test was continued until specimen fracture occurred or until 10^7 cycles were reached, which was considered the run-out limit. This method allowed assessment of the composite's resistance to repeated flexural stresses and its fatigue endurance limit.

Creep strength

Creep testing was conducted according to ASTM D2990 to determine the time-dependent deformation characteristics under constant tensile load. Specimens were subjected to constant stress levels of 20%, 30%, and 40% of the UTS at room temperature (≈25 °C). Axial elongation was measured continuously using an extensometer over a duration of 100 h. The collected strain-time data provided insight into the primary, secondary, and tertiary creep regions, enabling evaluation of the composite's long-term load-bearing capacity.

Water absorption behaviour

Water absorption tests were performed following ASTM D570. Specimens were oven-dried at 60 °C for 24 h, cooled in a desiccator, and weighed to obtain the initial dry weight (W_0). They were then fully immersed in distilled water at room temperature (≈25 °C). At predetermined intervals (2 h, 6 h, 12 h, 24 h, 48 h, 72 h, and every 24 h thereafter up to 7 days), and the specimens were weighed (*Wt*). The water absorption (%) was calculated using:

$$Water\ absorption\ (\%) = \frac{W_t - W_0}{W_0} \times 100$$

This procedure enabled quantification of the composite's hydrophilicity and evaluation of its dimensional stability in humid or wet environments.

Analysis of testing result

Examination of mechanical properties

Figure 6 presents the mechanical properties of areca nut fiber reinforced epoxy composites under varying loading conditions, including tensile strength, flexural strength, impact strength, and Shore-D hardness. The neat epoxy resin sample (R) exhibited the lowest performance, with a tensile strength of 65 ± 1.2 MPa, flexural strength of 94 ± 1.3 MPa, impact energy of 3.1 ± 0.1 J, and Shore-D hardness of 75 ± 1.1. These low values are attributed to the brittle nature of epoxy resin and its low elongation at break, which make it prone to cracking under stress [15].

The composite RA, containing 30 vol% areca nut fibers, displayed a tensile strength of 107 ± 1.4 MPa, representing a 64.6% increase compared to R. Flexural strength improved to 113 ± 1.5 MPa (20.2% increase), impact energy reached 3.5 ± 0.1 J (12.9% increase), and Shore-D hardness increased to 80 ± 1.3 (6.66% increase). This improvement is attributed to the fiber's ability to bridge cracks, limit deformation, and distribute loads effectively, along with strong fiber–matrix adhesion, which improves stress transfer and overall toughness [16, 17].

For pectin-containing composites, RAP0 (1 vol% pectin) achieved a tensile strength of 119 ± 1.5 MPa, an 11.2% increase compared to RA, and a 83.1% increase compared to R. Flexural strength reached 137 ± 1.6 MPa (21.2% higher than RA), impact energy increased to 4.1 ± 0.2 J (17.1% higher than RA), and Shore-D hardness

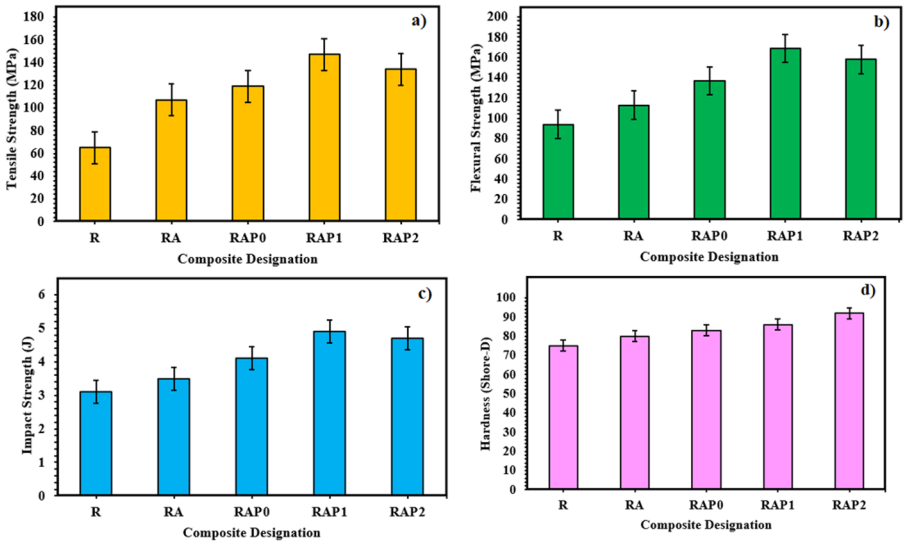

Fig. 6 Composites' mechanical properties

improved to 83.6 ± 1.4 (4.5% higher than RA). RAP1 (3 vol% pectin) showed further improvements, with tensile strength of 147 ± 1.6 MPa (37.4% increase vs. RA), flexural strength of 169 ± 1.7 MPa (49.5% increase vs. RA), impact strength of 4.9 ± 0.2 J (40% increase vs. RA), and Shore-D hardness of 86.6 ± 1.5 (8.25% increase vs. RA). These enhancements are attributed to pectin's ability to improve stress distribution, form hydrogen bonds with fiber surfaces, and create a more continuous matrix that enhances both flexibility and toughness [18, 19].

However, RAP2 (5 vol% pectin) showed a tensile strength of 134 ± 1.6 MPa, flexural strength of 158 ± 1.8 MPa, and impact energy of 4.7 ± 0.2 J, which represent decreases of 8.8%, 6.5%, and 4.08% respectively compared to RAP1, although still higher than R by 106%, 68%, and 51.6%. This decline is attributed to particle agglomeration at higher pectin loading, which introduces weak zones and stress concentration sites that reduce interfacial adhesion [17]. Shore-D hardness continued to increase, reaching 92 ± 1.9 (22.6% higher than R), due to the stiffness of the filler materials.

The SEM analysis (Fig. 7) provides further insights into these mechanical trends. Images at magnifications of 500× and 2.50 kx revealed that the R and RA samples (Fig. 7a) exhibited micro-voids and fiber pull-outs, indicating localized fiber debonding and insufficient stress transfer. In RAP0 and RAP1 (Fig. 7b and c), pectin particles were uniformly distributed within the matrix with minimal void formation, suggesting strong particle–matrix bonding. The smooth encapsulation of fibers and the presence of well-integrated pectin indicated effective load transfer and crack

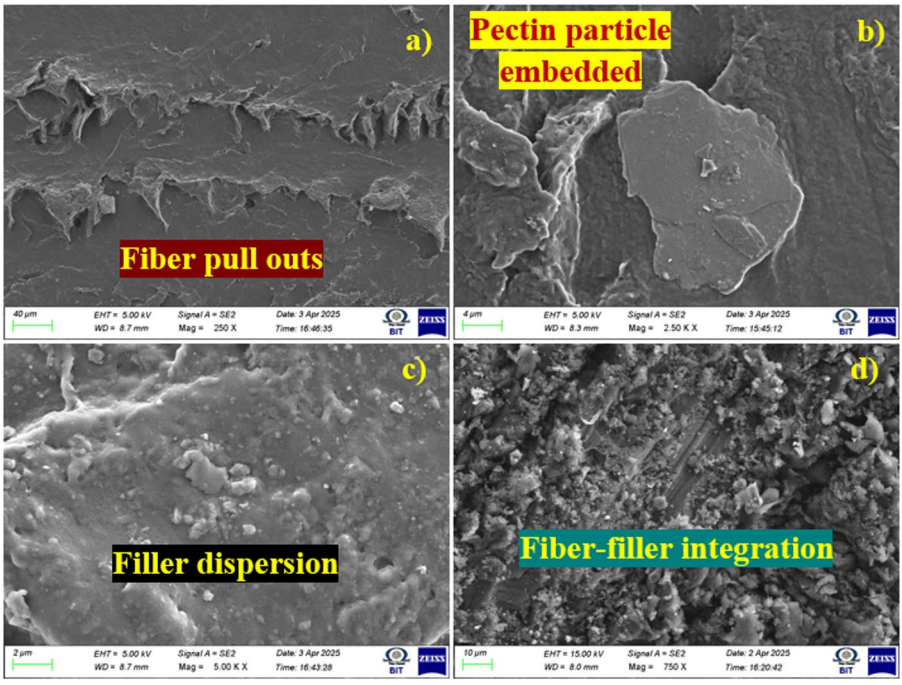

Fig. 7 Composites SEM examination

bridging. For RAP1, silane treatment resulted in a more uniform dispersion of pectin particles across the matrix, further minimizing interfacial defects. In RAP2 (Fig. 7d), higher pectin content led to visible particle agglomeration and roughened fracture surfaces, with clusters of fibers and filler that likely contributed to reduced tensile and flexural performance. Overall, SEM observations confirm that optimal pectin loading promotes uniform particle distribution, improved interfacial adhesion, and enhanced load-bearing capacity, whereas excessive loading can lead to agglomeration-related defects.

Evaluation of fatigue properties

The fatigue behavior of the composites was assessed using a rotational bending fatigue test machine at room temperature, in accordance with ASTM D3479. The tests were conducted at a constant stress ratio ($R = 0.1$), a loading frequency of 8 Hz, and under ambient laboratory conditions (27 ± 2 °C, relative humidity 50–55%). Three load levels corresponding to 25%, 50%, and 75% of the ultimate tensile strength (UTS) were applied to determine the number of cycles to failure. Each test was performed on three specimens per group, and the average values with standard deviations (± 1.1–1.9) were reported.At 25% UTS, the unreinforced epoxy resin (R) failed after 17,981 ± 1.5 cycles; at 50% UTS, after 16,551 ± 1.4 cycles; and at 75% UTS, after 15,515 ± 1.6 cycles, representing the lowest fatigue life among all samples. The reduced performance is attributed to the absence of reinforcement and the presence of micro-voids, which limited the ability to absorb and redistribute cyclic stresses.

Silane-treated areca nut fiber composites (RA) showed improved fatigue resistance, with 18,316 ± 1.3 cycles (25% UTS), 17,958 ± 1.5 cycles (50% UTS), and 16,851 ± 1.4 cycles (75% UTS). The enhancement is due to improved interfacial adhesion from silane functionalization, which promotes covalent bonding between fiber and matrix, reducing microcrack initiation and interfacial debonding during cyclic loading [19].The addition of pectin further enhanced performance. RAP0 (1 vol% pectin) exhibited 25,521 ± 1.4 cycles (25% UTS), 24,188 ± 1.7 cycles (50% UTS), and 23,781 ± 1.6 cycles (75% UTS). RAP1 (3 vol% pectin) achieved the highest fatigue life, with 28,781 ± 1.3 cycles (25% UTS), 27,517 ± 1.5 cycles (50% UTS), and 26,995 ± 1.4 cycles (75% UTS), representing an increase of 57–74% compared to RA. This superior performance is attributed to a balanced filler content, uniform dispersion of silane-treated particles, and optimal stress transfer, which collectively enhance energy absorption and delay crack propagation.

RAP2 (5 vol% pectin) displayed slightly reduced fatigue life at 27,184 ± 1.5 cycles (25% UTS), 26,885 ± 1.6 cycles (50% UTS), and 26,135 ± 1.7 cycles (75% UTS). The decline is likely due to filler agglomeration at higher loadings, which disrupts the polymer matrix continuity and acts as defect initiation sites, reducing deformability and cyclic energy absorption capacity. The observed failure modes under SEM included matrix cracking, fiber pull-out, and localized fiber–matrix debonding in R and RA specimens. RAP0 and RAP1 exhibited fewer pull-outs and smaller crack widths, indicating improved interfacial bonding. RAP2 showed micro-void clustering near agglomerates, which acted as fatigue crack initiation points. The fatigue life results for all composites are presented in Fig. 8.

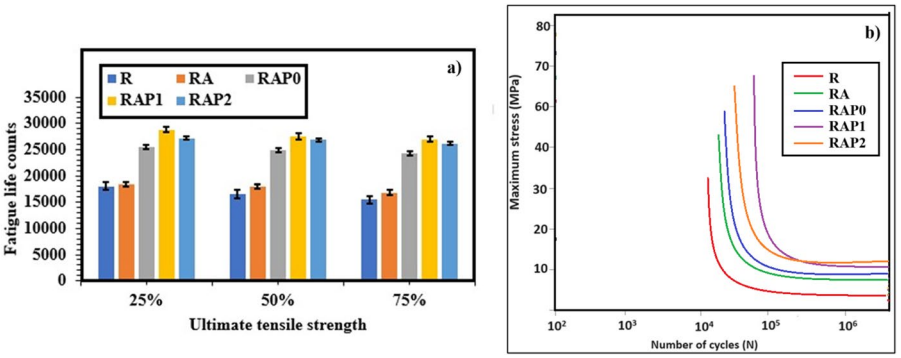

Fig. 8 (**a**) Fatigue life countsand (**b**) S-N curve for the composites that were prepared

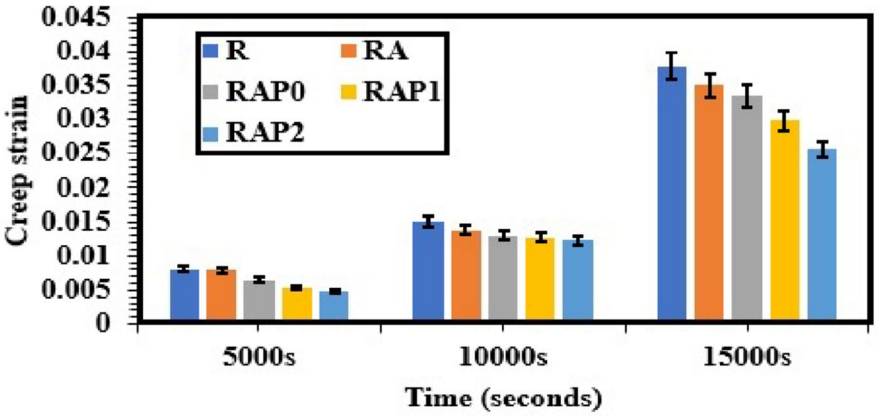

Fig. 9 Test analysis of creep behavior of the composite

Evaluation of creep properties

Figure 9 displays the creep behavior of the composites under a constant tensile load of 10 MPa, measured using a contact extensometer with 0.001 mm resolution. At times of 5000, 10,000, and 15,000 s, the creep strain values for the base resin sample (R) are 0.0081 ± 0.0002, 0.0150 ± 0.0003, and 0.0378 ± 0.0005, respectively. This behavior is attributed to the amorphous polymer's molecular chain relaxation under prolonged stress, where chain segments gradually reorient and slip past each other, leading to time-dependent deformation [20]. Composite RA, containing fibers, exhibits slightly reduced creep strain values of 0.0079 ± 0.0002, 0.0138 ± 0.0003, and 0.0350 ± 0.0004 at the same time intervals. The presence of fibers partially restricts chain mobility, slowing the relaxation process that causes creep, as fiber-matrix interfaces act as anchoring points for the polymer chains [21]. Further improvement is observed in the pectin-filled composites RAP0, RAP1, and RAP2. At 5000, 10,000, and 15,000 s, RAP0 records 0.0065 ± 0.0001, 0.0130 ± 0.0002, and 0.0335 ± 0.0004; RAP1 shows 0.0054 ± 0.0001, 0.0128 ± 0.0002, and 0.0298 ± 0.0003; and RAP2

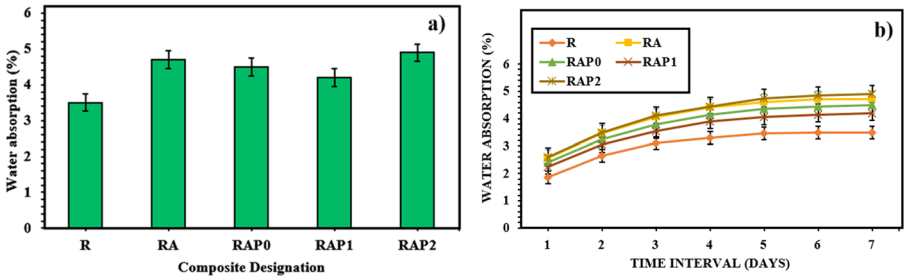

Fig. 10 Water absorption behavior of the composite

achieves the lowest creep strain values of 0.0048 ± 0.0001, 0.0123 ± 0.0002, and 0.0256 ± 0.0003, respectively. The reduced creep strain is linked to the dual role of pectin: it reinforces the matrix through physical entanglement and hydrogen bonding, and it promotes better stress transfer between fibers and matrix. These effects hinder chain slippage, limit free volume expansion, and reduce localized molecular mobility. Additionally, improved fiber-matrix interfacial adhesion minimizes microvoid growth and structural relaxation, enhancing the composite's long-term dimensional stability under sustained loading [22].

Evaluation of water absorption

In order to assess their longevity, dimensional stability, and functionality in damp or humid conditions, polymer composites undergo water absorption analysis. Figure 10 presents the water absorption behavior of epoxy composites. The base sample R, composed of pure epoxy resin, absorbed 3.5% water due to its densely crosslinked molecular structure, which limits the passage of water molecules. Its inherent hydrophobicity also helps maintain dimensional stability and prevents moisture-induced degradation [23]. With the incorporation of areca nut fiber, the water absorption in composite RA increased to 4.7% because the cellulose-rich fibers are hydrophilic, readily absorbing moisture. These fibers increase the number of accessible channels and sites for water uptake [24].

Composites RAP0 and RAP1 exhibited reduced water absorption of 4.5% and 4.2%, respectively, compared to RA when pectin was added at 1 and 3 vol%. At these low concentrations, pectin fills micro-voids in the matrix, creating a denser structure that limits water penetration. Additionally, improved fiber–matrix adhesion leaves less interfacial space for water ingress.

However, at a higher pectin loading of 5 vol% (RAP2), water absorption increased to 4.9%. This is because pectin, being a hydrophilic polysaccharide, contains abundant polar –OH groups that readily bind water. At high concentrations, excess pectin can agglomerate, disrupting matrix homogeneity and creating micro-voids, which in turn provide pathways for water infiltration [25]. Thus, pectin plays a dual role: at low content, it acts as a void-filling barrier to moisture, but at high content, its hydrophilicity and agglomeration promote water uptake.

Conclusion

This study examined epoxy composites reinforced with silane-treated areca nut fiber and pectin extracted from *Passiflora edulis* husks, focusing on mechanical, water absorption, fatigue, and creep behaviors. The key findings are:

- The RAP1 composite (30 vol% silane-treated fiber + 3 vol% silane-treated pectin) showed the highest mechanical performance, achieving tensile strength of 149 MPa, flexural strength of 169 MPa, and impact strength of 4.9 J.
- RAP1 exhibited excellent fatigue resistance with 27,517 failure cycles at 25% UTS and 26,995 cycles at 75% UTS.
- Improved interfacial bonding and uniform filler dispersion due to silane treatment enhanced stress transfer and reduced stress concentrations, contributing to the superior performance.
- The RAP2 composite (5 vol% silane-treated filler) recorded the highest hardness (92 Shore-D) but also the highest water absorption (4.9%) due to filler agglomeration.
- Silane treatment reduced overall water absorption by forming a hydrophobic coating on the reinforcements.
- RAP2 demonstrated outstanding creep resistance, with strains of 0.0048 at 5000 s, 0.0123 at 10,000 s, and 0.0256 at 15,000 s.

Limitation

This study did not evaluate the composites' durability under environmental aging conditions such as prolonged UV exposure, cyclic humidity–temperature fluctuations, or biological degradation. These factors may significantly influence long-term mechanical integrity, moisture resistance, and overall service-life performance.

Future recommendations

Further research should explore long-term durability under cyclic moisture–thermal conditions, optimization of filler dispersion techniques to minimize agglomeration, and scaling up the fabrication process for industrial applications in marine, construction, and lightweight automotive components.

Author contributions R. Ashok Gandhi - Conceptualization and writing of draft. V. Jayaseelan - Investigation. S. Sambath - Investigation. VijayAnanth Suyamburajan - Conceptualization. All authors equally contributed.

Funding No funding.

Data availability No datasets were generated or analysed during the current study.

Declarations

Competing interests The authors declare no competing interests.

Ethical approval The present study declaration form is represented below. In this study the ethical approval is not available and no competing interests are present. Further consent to participate and consent to publish is present.

References

1. Nag MK, Shrivastava A (2024) *Proceedings of the Institution of Mechanical Engineers, Part E: Journal of Process Mechanical Engineering*, 09544089241226762. https://doi.org/10.1177/09544089241226762
2. Ramanan G, RS RI, Suresh S, Singh P, Paavana M, Sneha SK, Raja V (2025) Results Eng 25. https://doi.org/10.1016/j.rineng.2025.104474
3. Natarajan S, Pathinettampadian G, Vadivel M, Yesudasan PSS, Jesuretnam BR (2022) J Nat Fibers 19(15):12004–12014. https://doi.org/10.1080/15440478.2022.2048942
4. Nag MK (2024) J Stored Prod Res 106:102290. https://doi.org/10.1016/j.jspr.2024.102290
5. Nag MK, Kumar P, Nayak S, Shrivastava A (2022), December In *International conference on sustainable technologies and advances in automation, aerospace and robotics* (pp. 471–481). Singapore: Springer Nature Singapore. https://doi.org/10.1007/978-981-99-2349-6_43
6. Nag MK, Shrivastava A, Solanki K (2022) Int J Therm Energy Appl 8(2):1–8. https://doi.org/10.37628/ijtea.v8i2.1490
7. Nag MK (2023) Int J Sci Res Eng Manage (IJSREM) 7(3):1–4. https://doi.org/10.55041/IJSREM18461
8. Balguri PK, Latha A, Kaur L, Verma R, Kumar DS, Ramasree S, Nagabhooshanam N (2024) Biomass Conversion and Biorefinery, 1–11. https://doi.org/10.1007/s13399-024-06088-x
9. Anžlovar A, Krajnc A, Žagar E (2020) Cellulose 27:5785–5800. https://doi.org/10.1007/s10570-020-03181-y
10. Nayak S, Nag MK, Shrivastava A, Paswan M (2022), December In *International conference on sustainable technologies and advances in automation, aerospace and robotics* (pp. 385–394). Singapore: Springer Nature Singapore. https://doi.org/10.1007/978-981-99-2349-6_35
11. Mohankumar D, Amarnath V, Bhuvaneswari V, Saran SP, Saravanaraj K, Gogul MS, Rajeshkumar L (2021) AprilIn IOP conference series: materials science and engineering (Vol. 1145, No. 1, p. 012023). IOP Publishing. https://doi.org/10.1088/1757-899X/1145/1/012023
12. Khubber S, Kazemi M, AmiriSamani S, Lorenzo JM, Simal-Gandara J, Barba FJ (2023) Food Reviews Int 39(4):2352–2377. https://doi.org/10.1080/87559129.2021.1952422
13. Vishal K, Rajkumar K, Nitin MS, Sabarinathan P International Journal of Biological Macromolecules, 209, 1248–1259., Nag MK, Kumar P (2022) (2024). *Proceedings of the Institution of Mechanical Engineers, Part L: Journal of Materials: Design and Applications*, *238*(1), 73–99. https://doi.org/10.1177/14644207231183966
14. Nag MK, and Kumar P (2024). Proceedings of the Institution of Mechanical Engineers, Part L: Journal of Materials: Design and Applications, 238(1), 73-99. https://doi.org/10.1177/14644207231183966
15. Atmakuri A, Palevicius A, Vilkauskas A, Janusas G (2022) Polymers 14(13):2612. https://doi.org/10.3390/polym14132612
16. Nag MK, Kumar P (2024) J Mech Sci Technol 38(11):6075–6084. https://doi.org/10.1007/s12206-024-1025-9
17. Ramakrishnan T, Senthil Kumar S, Samuel Chelladurai SJ, Gnanasekaran S, Geetha NK, Arthanari R, Debtera B (2022) Advances in Materials Science and Engineering, 2022(1), 3533143. https://doi.org/10.1155/2022/3533143
18. Nag MK (2025) Iran Polym J 34(2):259–275. https://doi.org/10.1007/s13726-024-01378-7
19. Musthaq MA, Dhakal HN, Zhang Z, Barouni A, Zahari R (2023) Polymers 15(5):1229. https://doi.org/10.3390/polym15051229
19. Barouni A, Lupton C, Jiang C, Saifullah A, Giasin K, Zhang Z, Dhakal HN (2022) Compos Struct 281:115046. https://doi.org/10.1016/j.compstruct.2021.115046
20. Nag M, Kumar K (2023) Proc Institution Mech Eng Part C: J Mech Eng Sci 237(16):3630–3649. https://doi.org/10.1177/09544062221149388
21. Katouzian M, Vlase S, Marin M, Öchsner A (2022) Discover Mech Eng 1(1):3. https://doi.org/10.1007/s44245-022-00003-2

22. Battawi AA, Abed BH (2023) J Theor Appl Mech 53. https://doi.org/10.55787/jtams.23.53.2.136
23. Kchaou M, Arul SJ, Athijayamani A, Adhikary P, Murugan S, Aldawood FK, Abualkhair HF (2023) Mater Science-Poland 41(4):132–143. https://doi.org/10.2478/msp-2023-001
24. Nag MK, Kumar P, Paswan MK (2020) In *Recent advances in power systems: select proceedings of EPREC 2020* (pp. 453–465). Singapore: Springer Singapore. https://doi.org/10.1007/978-981-15-7994-3_42
25. Ng LF, Yahya MY, Muthukumar C (2022) Polym Compos 43(1):203–214. https://doi.org/10.1002/pc.26367